Volume 44 | Number 10 | 21 May 2015 | Pages 2789–3348

Chem Soc Rev

Chemical Society Reviews
www.rsc.org/chemsocrev

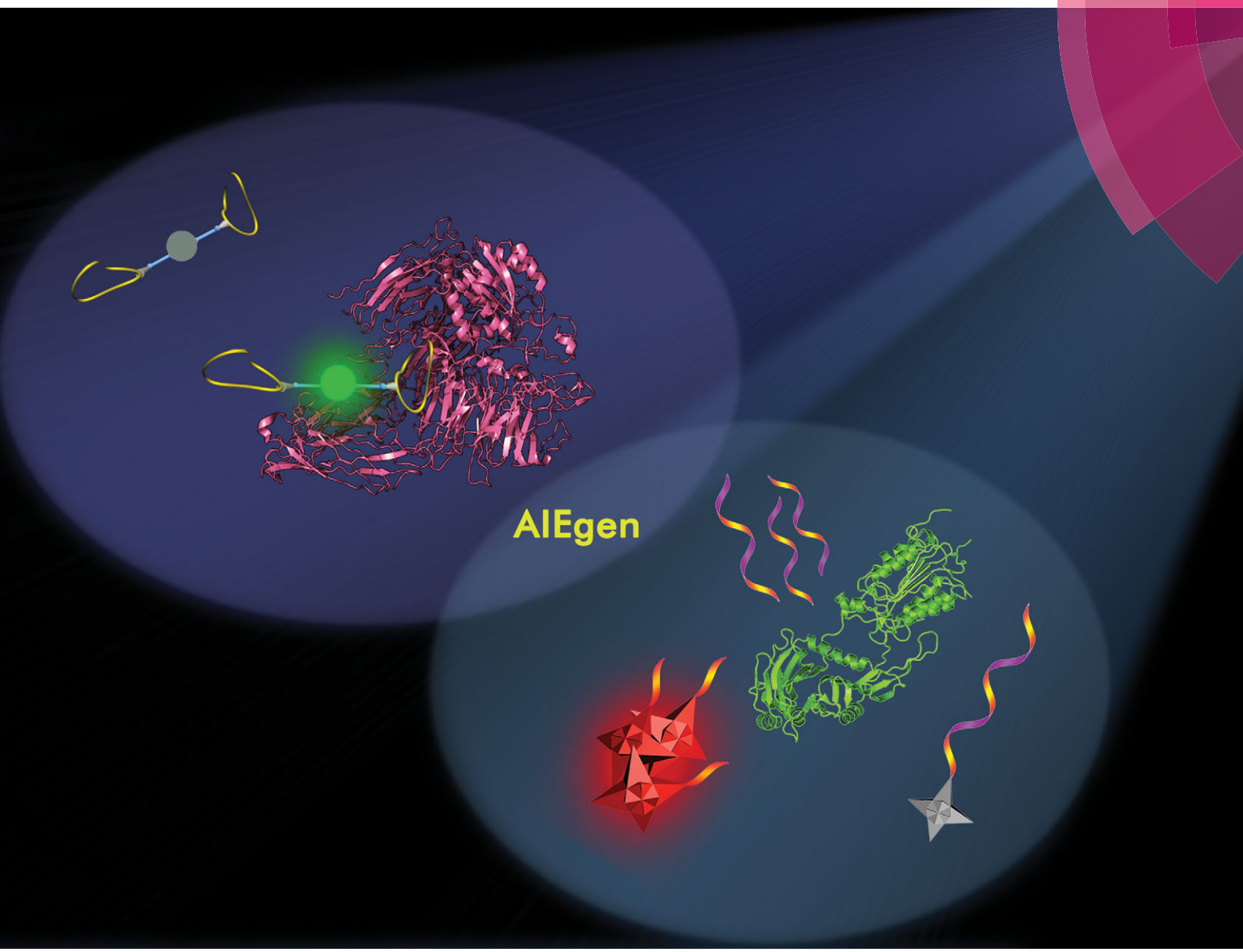

ISSN 0306-0012

ROYAL SOCIETY OF CHEMISTRY

TUTORIAL REVIEW
Ben Zhong Tang, Bin Liu *et al.*
Specific light-up bioprobes based on AIEgen conjugates

Chem Soc Rev

TUTORIAL REVIEW

View Article Online
View Journal | View Issue

Cite this: *Chem. Soc. Rev.*, 2015, 44, 2798

Specific light-up bioprobes based on AIEgen conjugates

Jing Liang,[ab] Ben Zhong Tang*[cd] and Bin Liu*[ae]

Received 1st December 2014

DOI: 10.1039/c4cs00444b

www.rsc.org/csr

Driven by the high demand for sensitive and specific tools for optical sensing and imaging, bioprobes with various working mechanisms and advanced functionalities are flourishing at an incredible speed. Conventional fluorescent probes suffer from the notorious effect of aggregation-caused quenching that imposes limitation on their labelling efficiency or concentration to achieve desired sensitivity. The recently emerged fluorogens with an aggregation-induced emission (AIE) feature offer a timely remedy to tackle the challenge. Utilizing the unique properties of AIE fluorogens (AIEgens), specific light-up probes have been constructed through functionalization with recognition elements, showing advantages such as low background interference, a high signal to noise ratio and superior photostability with activatable therapeutic effects. In this tutorial review, we summarize the recent progress in the development of specific AIEgen-based light-up bioprobes. Through illustration of their operation mechanisms and application examples, we hope to provide guidelines for the design of more advanced AIE sensing and imaging platforms with high selectivity, great sensitivity and wide adaptability to a broad range of biomedical applications.

Key learning points
- Concept of aggregation induced emission (AIE) and its working mechanism.
- Common functionalization techniques of AIEgens to yield specific light-up bioprobes.
- Overall design principles and operation mechanisms of specific AIE light-up bioprobes.
- Examples of specific AIE light-up probes and their biomedical applications.

1. Introduction

Fluorescent probes are undoubtedly some of the most promising tools for real-time, on-site and non-invasive visualization of biological molecules and processes in live cells and organisms. The probes not only provide valuable insights in understanding physiological alterations in pathological settings but also serve as useful tools for the development of personalized medicine and targeted therapies. Sensitivity of bioprobes, which is determined by the signal-to-noise ratio (SNR), is of utmost importance as many biological processes involve only minute changes in biochemical species. Although a wide array of fluorescent bioprobes have been developed, many of them comprise a targeting ligand and a conventional fluorophore, which are intrinsically fluorescent with high background signals. In addition, they usually suffer from the notorious aggregation-caused quenching effect, which prohibits them from being used at high concentrations that leads to reduced fluorescence and compromised sensitivity. Amongst the many fluorescent bioprobes, light-up probes are especially attractive due to their reduced false-positive responses as compared to their turn-off counterparts. Typical light-up probes usually involve photoinduced electron transfer, internal charge transfer or energy transfer mechanisms.[1] Fluorogenic dyes or dual-labelled bioprobes with emitter–quencher pairs are especially common for monitoring enzyme–substrate interactions and DNA hybridization in which the separation of the emitter and quencher results in restored fluorescence.[2,3]

The discovery of a novel class of fluorogenic molecules with aggregation-induced emission (AIE) characteristics has sparked

[a] *Department of Chemical and Biomolecular Engineering, 4 Engineering Drive 4, National University of Singapore (NUS), Singapore 117585*
[b] *NUS Environmental Research Institute, 5A Engineering Drive 1, Singapore 117411*
[c] *Department of Chemistry, Institute of Molecular Functional Materials and Division of Life Sciences, The Hong Kong University of Science and Technology (HKUST), Clear Water Bay, Kowloon, Hong Kong, China. E-mail: tangbenz@ust.hk*
[d] *SCUT-HKUST Joint Research Laboratory, State Key Laboratory of Luminescent Materials and Devices, South China University of Technology (SCUT), Guangzhou, China 510640*
[e] *Institute of Materials Research and Engineering (A*STAR), 3 Research Link, Singapore 117602. E-mail: cheliub@nus.edu.sg*

intense research interest in the design and synthesis of AIE probes for biosensing and imaging applications. Different from conventional fluorophores, AIE fluorogens (AIEgens) are nearly non-emissive in the molecular state but emit strongly in the aggregated state. These fluorogens can be engineered to show extremely weak fluorescence in aqueous media by endowing them with water solubility, so that they can be compatible with biological systems, with their fluorescence being turned on upon interacting with target analytes. As fluorescence signals of AIE probes are generated only when their intermolecular rotations are restricted or upon aggregate formation, AIE probes offer higher resistance to photobleaching and thus superior photostability and higher signal reliability relative to conventional probes. Furthermore, the very low background of AIEgen light-up bioprobes renders them especially attractive in continuous monitoring of biological processes without the need of repeated washing steps.

The identification of specific molecular species and the study of biological events rely heavily on the selectivity of the probes. Earlier work reported on cationic and anionic AIEgens which showed light-up responses to a variety of analytes, such as nucleic acids, proteins, and small molecules.[4,5] However, the probe–analyte interactions based on electrostatic or hydrophobic forces make them less useful in complex media containing a large amount of interfering substances. The selectivity of the bioprobe can be significantly improved by conjugation with recognition elements that have specific affinity for the analytes of interest. It is also possible to incorporate other functional elements such as prodrugs to develop image-guided therapeutic probes. The major challenge of designing specific AIEgen light-up bioprobes is to introduce recognition elements or functional units that are compatible with the conjugation reactions while maintaining their low background and good light-up potential.

This review gives an account of the recent development of specific light-up bioprobes based on AIEgens. Typical AIEgens and common bioconjugation techniques are introduced first, followed by the operation mechanisms and design rationale of the probes. In the following section, examples of specific light-up AIE bioprobes for various applications are demonstrated, which include specific molecular detection, targeted cell imaging, controlled and selective drug delivery, on-demand therapy, enzyme activity assay and bacterial inhibition. This review is organized according to the type of recognition elements conjugated to AIEgens, which include nucleic acids, peptides and small molecule ligands. In each section, the discussion is further elaborated according to target analytes or specific applications. Mastering the art of AIE probe design and synthesis not only aids in the development of highly sensitive and selective bioprobes, but also opens up endless opportunities for AIEgens to be used as versatile tools for potential clinical diagnostic and disease therapeutic applications.

2. AIEgens and functionalization

Since the discovery of the first silole compound hexaphenylsilole (HPS) that exhibits AIE phenomenon,[6] a substantial number of AIEgens have emerged.[7,8] They share the common

Jing Liang

Jing Liang received her PhD degree in Chemical Engineering from the National University of Singapore in 2013. She is currently a postdoctoral researcher in Prof. Bin Liu's research group in the Department of Chemical and Biomolecular Engineering. Her research interests include biosensing and bioimaging based on conjugated polymers, aggregation-induced emission fluorogens and noble metal nanomaterials.

Ben Zhong Tang

Ben Zhong Tang received his PhD degree from Kyoto University and conducted his postdoctoral work at the University of Toronto. He is Chair Professor in the Department of Chemistry and Division of Biomedical Engineering, Stephen K. C. Cheong Professor of Science at HKUST, and also a honorary professor at SCUT. He was elected to the Chinese Academy of Sciences in 2009. His research interest lies in the creation of new molecules with novel structures and unique properties with implications for high-tech applications. He is currently an Associate Editor of Polymer Chemistry and is on the editorial board of a dozen journals.

Bin Liu

Bin Liu received her PhD degree in Chemistry from the National University of Singapore in 2001. After postdoctoral training at the University of California Santa Barbara, she joined NUS where she is currently an associate professor in the Department of Chemical and Biomolecular Engineering. Her research focuses on the design and synthesis of functional water-soluble conjugated polymers and organic nanomaterials and exploration of their applications in sensors, imaging and optoelectronic devices. She is serving as Associate Editor of Polymer Chemistry.

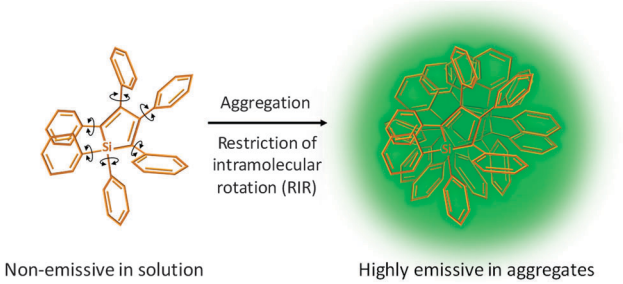

Scheme 1 Schematic illustration of the AIE phenomenon using HPS as an example.

structural feature with propeller shaped phenyl rings that can rotate freely in good solvents to result in annihilated emission. Upon restriction of intramolecular rotation (RIR) of such fluorogens, the radiative decay channel is activated, which leads to highly emissive states (Scheme 1).

Among the AIEgens, tetraphenylethene (TPE) and tetraphenylsilole (TPS) derivatives have gained the most popularity in the construction of AIE bioprobes. Although the short wavelength has restricted their use in *in vivo* studies, the design principle of TPE/TPS-based probes can be easily generalized to other types of AIEgens with a more amiable emission range.

While ionic groups such as ammonium and sulfonate have been frequently introduced into AIEgens for direct binding with charged analytes, more specific targeting ligands can be conjugated to AIEgens *via* simple coupling chemistry between the functional groups of the two moieties. Scheme 2 lists a summary of common conjugation chemistry to yield AIE conjugates. The copper(I)-catalyzed "click chemistry" between azide and alkyne is one of the most widely used conjugation methods due to its bioorthogonality and rapid reaction kinetics that can lead to efficient coupling with minimum side reactions (Scheme 2A).[9] Peptides and small molecules have been widely modified with an azido or an alkyne group for conjugation with their AIE counterparts. For ligands that contain primary amine groups, isothiocyanate (NCS) or carboxyl group functionalized AIEgens could be used for conjugation (Scheme 2B and C). The latter is a widely used coupling method due to the abundance of amine groups in peptides or proteins, which usually requires activation of carboxyl group with 1-ethyl-3-(-3-dimethylaminopropyl) carbodiimide hydrochloride (EDC) and *N*-hydroxysulfosuccinimide sodium salt (sulfo-NHS) for efficient coupling. The primary amine-functionalized AIEgen can be directly coupled with reactive *N*-hydroxysuccinimide (NHS) ester containing compounds, creating a stable amide linkage between the AIEgen and the recognition element (Scheme 2D). Another popular method for conjugation involves the maleimide with thiol which yields a stable thioester bond (Scheme 2E). This reaction proceeds rapidly and is especially useful for conjugation between cysteine containing peptides and maleimide functionalized AIEgens.

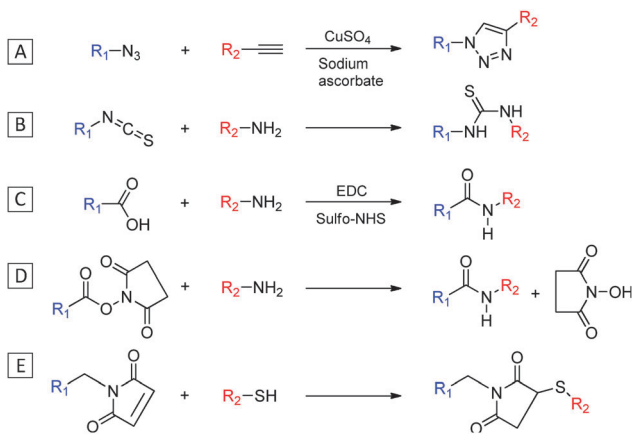

Scheme 2 Typical coupling reactions between functionalized AIEgens and recognition elements.

3. Specific AIE light-up bioprobes

3.1 Probe design principles and operation mechanisms

As the fluorescence generation of traditional AIEgens is attributed to RIR, the key to AIE light-up probes is to ensure their low background signal and the activation of the AIE mechanism in response to specific analytes. The majority of specific AIE light-up bioprobes operate in two mechanisms: through direct binding with a specific target or site specific reaction due to the presence of the target analyte (Scheme 3). In the first mechanism, an AIEgen is conjugated with a targeting ligand that can selectively bind to the analyte of interest which induces restriction of molecular motions of the probe to turn on the fluorescence (Scheme 3A). The recognition ligands attached are preferably molecules with small molecular weights as conjugation of very large molecules may hinder the molecular motions of the probe to produce a high background signal and result in insensitive response to target binding. In the second mechanism, an AIEgen is functionalized with a ligand which undergoes a reaction (*e.g.* enzymatic cleavage by the target molecule) to yield a product that can form highly emissive aggregates (Scheme 3B). While the first mechanism is highly desirable for biomarker detection, the second one is especially useful for sensing enzymes or other molecules that undergo cleavage reactions with the probe.

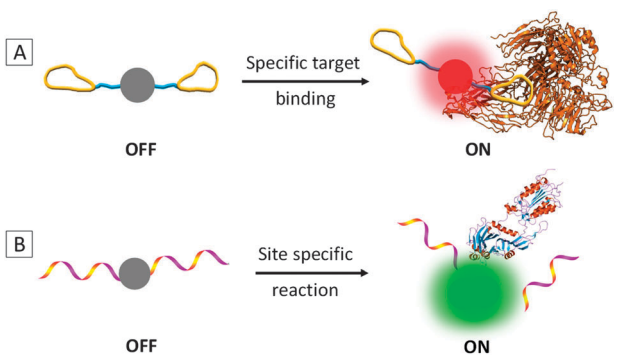

Scheme 3 Schematic illustration of typical light-up mechanisms for specific AIE bioprobes.

Based on the above two mechanisms, three generations of specific AIE light-up bioprobes have been reported thus far. The first generation has a very simple structure of an AIEgen directly linked to a water-soluble recognition element. The good water-solubility of the recognition element is essential to bring the probes into aqueous media with minimized self-aggregation to ensure a low fluorescence background. In reality, however, the recognition elements for many target analytes have limited water solubility, which are not suitable for direct conjugation to AIEgens. One solution to this challenge is to introduce hydrophilic elements into the probes to improve their overall water solubility so as to achieve a low background signal and a high light-up ratio. The second generation probe thus includes three parts: an AIEgen, a hydrophilic linker (*e.g.* short peptides) and a specific recognition element. As compared to the first generation, the probe design for the second generation is more general, which has successfully expanded the recognition elements to both hydrophilic and hydrophobic ones. In both cases, good water solubility of the probe is a prerequisite condition, which poses constraints to the nature and type of the recognition elements to be conjugated. In addition, the additional modification required for hydrophobic recognition elements may add complexity of the probe design and operation. To overcome this limitation, the third generation AIE light-up probes are designed based on fluorogens with both AIE and excited state intramolecular proton transfer (ESIPT) characteristics.[10] As the ESIPT process involves proton transfer in the excited state, it is strongly dependent on the intramolecular hydrogen bonding. The AIE + ESIPT probes are thus non-fluorescent once the hydrogen bonding is blocked. In addition to the light-up mechanisms of conventional AIE probes, the AIE + ESIPT design offers additional advantages of large Stokes shifts and easy operation with no limitation on probe solubility. It is worth noting that fluorophores with strong charge transfer characters were also found to exhibit the AIE phenomenon, but *via* a different mechanism.[11,12]

3.2 AIE–DNA conjugates

DNA strands are negatively charged macromolecules that carry important genetic information of all living organisms and viruses. Non-specific probes can be simply constructed using positively charged AIEgens that show light-up response to DNA due to complexation-induced aggregation. The ability to specifically probe the DNA sequence is crucial for genetic mapping, disease screening, oncology studies and so forth. By conjugating DNA strands to AIEgens, specific DNA probes can be created by taking advantages of the hybridization between complementary single stranded DNA (ssDNA).

In 2013, Häner's group investigated the control of AIE properties by DNA hybridization using dialkynyl-tetraphenylethylene (DATPE) modified DNA strands.[13] The two stereoisomers of DATPE building blocks (M_E and M_Z in Fig. 1A) were synthesized and separately incorporated into oligonucleotides (ONs) *via* automated oligomer synthesis. Complementary ON pairs with both one and two DATPE building blocks were allowed to hybridize and their optical properties were monitored. It was found that upon hybridization, the absorption maximum of the single strand (**ON1**: 5′-AGC TCG GTC AM$_E$C GAG AGT GCA) red-shifted from 327 nm to 335 nm of its duplex form (**D1**, hybrid of **ON1** and **ON2**) and the fluorescence of **D1** was significantly higher than its individual single strands due to molecular aggregation of the two M_E units. Similar effects were observed for **M$_z$-ON**. It was also found that the fluorescence of two DATPEs in duplex (**D2**, hybrid of **ON3** and **ON4**) was almost three-fold higher than that in the single strand (**ON7**) (Fig. 1B). The emissions of the hybridized ONs with two M_Es (**D3**, the hybrid of **ON5** and **ON6**) and two M_Zs (**D4**, the hybrid of **ON7** and **ON8**) were the highest, with respective quantum yields of 30.6% and 32.1%, comparable to those of the aggregated state of their DATPE building blocks (39.9% and 39.2% for *E*-DATPE and *Z*-DATPE, respectively). The findings indicated that the emission of AIE–DNA conjugates could be controlled by hybridization induced aggregation, making them promising as DNA light-up probes.

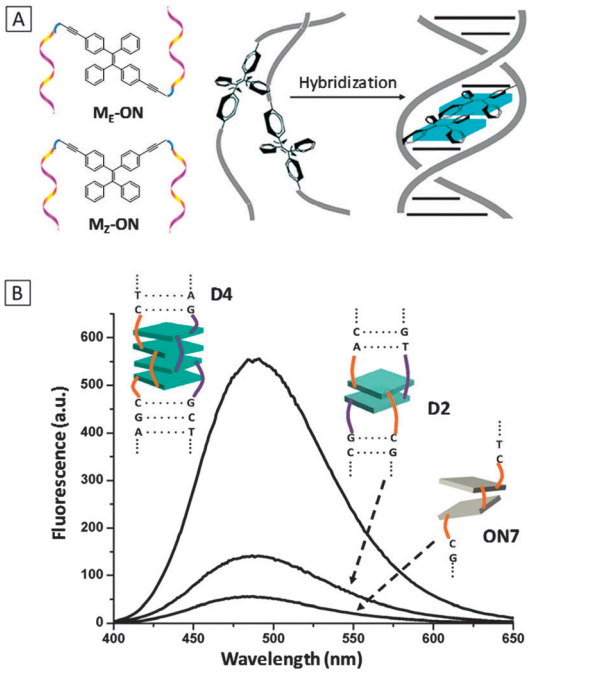

Fig. 1 (A) Schematic diagram of oligonucleotide-functionalized TPE in different configurations (**M$_E$-ON** and **M$_Z$-ON**) and a general scheme of fluorescence light-up upon hybridization. (B) Fluorescence spectra of hybridized complexes **D2**, **D4** and oligomer **ON7**. (λ_{ex} = 335 nm). **D2**: the hybrid of **ON3** (5′-AGC TCG GTC **AM$_z$**C GAG AGT GCA) and **ON4** (3′-TCG AGC CAG **TM$_z$**G CTC TCA CGT); **D4**: hybrid of **ON7** (5′-AGC TCG GTC **M$_z$Mz**C GAG AGT GCA) and **ON8** (3′-TCG AGC CAG **M$_z$Mz**G CTC TCA CGT). Adapted from ref. 13, and reprinted with permission from The Royal Society of Chemistry 2013.

The first light-up probe for detection of specific DNA sequence using AIE–DNA conjugates was recently reported.[14] The probe consists of a TPE fluorogen conjugated with a 20 mer ssDNA probe (DNA_p). Upon hybridization with the complementary DNA (DNA_t), the fluorescence of the probe increased by about three-fold, which could be explained by the increased rigidity and mass that inhibit rotational movement of the phenyl rings in TPE.

Further studies revealed that the emission of the perfectly hybridized duplex TPE–DNA_p–DNA_t was much higher than that of the probe hybridized with one and two mismatched strands. The selectivity over the perfectly matched strand indicated the probe's ability to detect single nucleotide polymorphism. A detection limit of 0.3 μM DNA_t was achieved.

In addition to conjugating DNA strands on AIEgens, a single nucleotide (thymine)-substituted TPE fluorogen was also developed for detection of adenine-rich ssDNA.[15] This probe took advantage of the specific reaction between thymine and adenine to form hydrogen bonds which induced aggregation of the probes along DNA strand to activate the AIE mechanism. The probe showed significantly higher light-up response to ssDNA as compared to double-stranded DNA (dsDNA), which is different from the conventional dsDNA intercalating dyes. The extent of fluorescence turn-on increased with the adenine content of the target DNA, indicating that the probe was useful for screening adenine content of ssDNA.

3.3 AIE–peptide conjugates

As the building blocks of proteins, peptides have become increasingly popular for design of fluorescent probes due to their small size, ease of synthesis and functionalization. Properly sequenced peptides can not only serve as probing ligands for protein biomarkers, enzymes and small molecules, but are also versatile linkers for fine-tuning the water-solubility of the probe.

3.3.1 Biomarker detection. In 2012, the first example of the AIE–peptide conjugate was reported for the specific detection of integrin, an important biomarker protein for many types of tumor cells.[16] The probe **TPS-2cRGD** (Fig. 2A) was synthesized *via* the click reaction between TPS fluorogen and the cyclic-RGD (cRGD) peptide, derived from extracellular matrix protein that has high affinity for integrin. As seen from the inset of Fig. 2B, the probe is non-emissive in DMSO/water (1 : 199 v/v) due to the good water solubility endowed by cRGD and its fluorescence is progressively turned on upon incubation with an increasing amount of integrin as a result of the RIR mechanism. The probe displayed the highest fluorescence light-up with integrin, which was up to 182-fold higher than other seven proteins, indicating high specificity of the probe (Fig. 2B). The detection limit was estimated to be 0.5 μg mL^{-1}. **TPS-2cRGD** was further utilized for imaging of live HeLa cells with overexpressed integrin on membranes (Fig. 2C) and a good overlap was observed with a commercial membrane tracker (Fig. 2D and E). Real-time tracking of integrin internalization was also performed over the course of 30 min. The excellent light-up ability and specificity of the probe makes it useful for identification of integrin-positive cells from integrin-negative ones. This work represents the first example of the AIE light-up probe for specific real-time biomarker imaging.

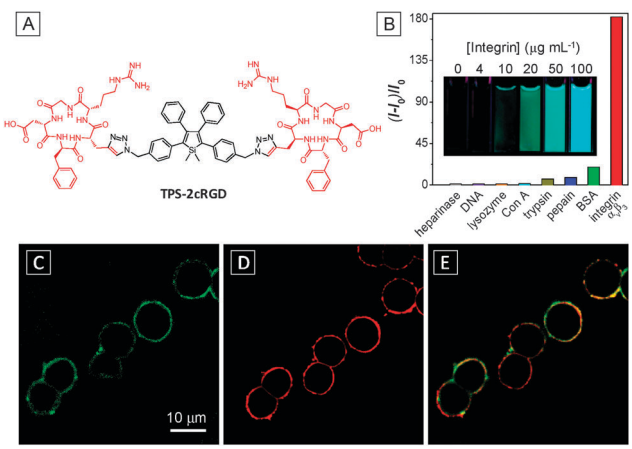

Fig. 2 (A) Chemical structure of **TPS-2cRGD**. (B) Plot of $(I\text{-}I_0)/I_0$ *versus* different proteins and DNA, where I and I_0 are the PL intensities at analyte concentrations of 100 and 0 μg mL^{-1}, respectively. Inset: photographs of the **TPS-2cRGD** probe in the presence of integrin at different concentrations under UV illumination. λ_{ex} = 365 nm. Confocal fluorescent images of live HeLa cells after staining with 2 μM **TPS-2cRGD** (C) and membrane tracker (62.5 ng mL^{-1}) (D) and their overlay image (E). **TPS-2cRGD**: λ_{ex} = 405 nm with filter band pass of 505–525 nm; membrane tracker: λ_{ex} = 543 nm with a filter band pass of 575–635 nm. Scale bar: 10 μm. Adapted from ref. 16, and reprinted with permission from American Chemical Society 2012.

3.3.2 Small molecule detection. As most of the recognition elements lack hydrophilicity, the development of the second generation light-up probes requires fine-tuning of the probe water-solubility to control their background signal. Liu's group has studied the optical properties of TPE conjugated with different numbers of the hydrophilic amino acids to reveal the importance of peptide design upon adjusting the fluorescence of AIEgen in aqueous media.[18] The TPE-peptide conjugates with 1–5 units of aspartic acids (D) were synthesized *via* the coupling reaction between TPE-NCS and the primary amine groups on the peptides (Fig. 3A). The fluorescence measurements

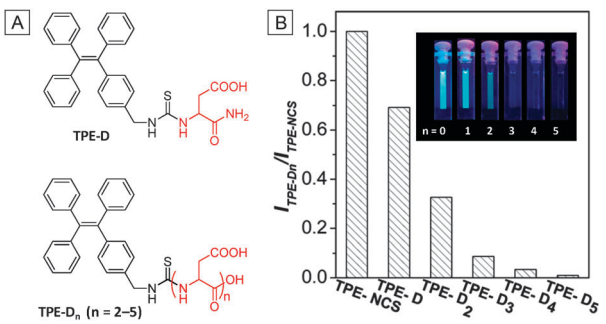

Fig. 3 (A) Chemical structures of **TPE-D_n**. (B) Ratios of PL intensities of **TPE-D_n** to TPE-NCS in DMSO/H_2O (v/v = 1/199). TPE-NCS: λ_{ex} = 314 nm; TPE-D_n: λ_{ex} = 304 nm; [TPE-NCS] = [**TPE-D_n**] = 10 μM. Inset: photographs of 10 μM **TPE-D_n** (n = 0–5) in DMSO/H_2O (v/v = 1 : 199) taken under UV light irradiation (λ_{ex} = 365 nm). Adapted from ref. 18 and reprinted with permission from American Chemical Society 2014.

of **TPE-D$_n$** (n = 1–5) and their hydrophobic precursor TPE-NCS in DMSO–water mixtures showed that the emission intensity correlated inversely with the number of Ds (Fig. 3B). The decreasing emission with an increasing number of Ds was attributed to improved water solubility that promoted better dispersion of the conjugates. Laser light scattering (LLS) revealed the presence of nanoaggregates in TPE conjugates with 0–3 units of Ds with decreasing sizes while no signal was collected for conjugates with 4 or 5 Ds. Five units of Ds were found to be the threshold to effectively turn off the fluorescence of TPE conjugates.

On the basis of the above findings, a light-up probe for thiol was designed and synthesized by attaching an additional targeting ligand for intracellular thiol imaging in specific cells.[19] As shown in Fig. 4A, the probe consists of a TPE conjugated with three segments, a thiol-cleavable disulfide linker dithiobis(succinimidyl propionate) (DSP), a hydrophilic linker with five Ds and a cRGD peptide which can selectively bind to integrin receptors in targeted cells. Upon integrin binding, the probe could be internalized by the cells which were subsequently cleaved by glutathione (GSH), the most abundant thiol in mammalian cells, to turn on the fluorescence. The detection limit of GSH in solution was reported to be 1.0 μM. Confocal fluorescence imaging studies showed that the fluorescence signal from integrin rich U87-MG cells (Fig. 4B) is much stronger than that in MCF-7 cells with low integrin expression (Fig. 4D). In comparison, the control conjugate of **TPE** linked to **D$_5$** *via* a disulfide linker (**TPE-SS-D$_5$**) showed weak fluorescence for both cell lines due to the lack of integrin receptor-mediated uptake (Fig. 4C and E). This probe design highlights the importance of both hydrophilic linker and targeting ligand for effective specific cell uptake and high SNR.

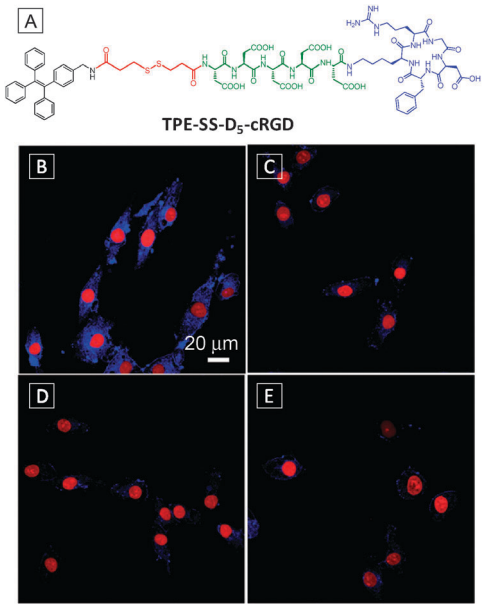

Fig. 4 (A) Chemical structure of **TPE-SS-D$_5$-cRGD**. Confocal fluorescence images of U87-MG (B, C) and MCF-7 (D, E) cells after incubation with **TPE-SS-D$_5$-cRGD** (B, D) and **TPE-SS-D$_5$** (C, E). The nuclei were stained with propidium iodide. Scale bar: 20 μm. Adapted from ref. 19, and reprinted with permission from The Royal Society of Chemistry 2014.

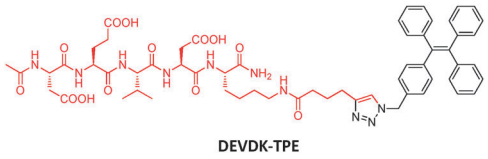

Scheme 4 Chemical structure of the **DEVDK-TPE** probe.

3.3.3 Apoptosis imaging. Apoptosis is a programmed cell death process that plays a critical role in regulating development and functions of multicellular organism. Real-time imaging of apoptosis has great implications in early diagnosis of diseases, monitoring of disease progression and drug screening. As an important regulator enzyme in the reaction cascade of the apoptosis pathway, caspase-3/7 has been identified as one of the key biomarkers for detecting apoptosis activation. The ability of caspase-3/7 to cleave a well-known peptide substrate Asp-Glu-Val-Asp (DEVD) has been used in the design of a number of AIE light-up probes based on the cleave-type mechanism. In addition, the hydrophilic nature of the substrates does not require additional modification, which simplifies probe design. The first example of the AIE light-up probe for apoptosis utilises a TPE conjugated with DEVDK peptides, which is water-soluble and almost non-emissive in aqueous media. The probe **DEVDK-TPE** (Scheme 4) could be selectively cleaved by caspase-3/7 *via* the D–K linkage to yield a highly emissive product.[20] The light-up ratios of the probe upon reaction with caspase-3 and -7 were 45 and 28, respectively, significantly higher than that induced by other interfering proteins. The kinetics study revealed that the probe outperformed two other commercial fluorogenic probes of Ac-DEVD-AFC and Z-DEVD-AFC. The probe was also proved effective for real-time monitoring of apoptosis and screening of apoptosis related drugs.

Despite the effectiveness of DEVDK-TPE in apoptosis imaging *in vitro*, the probe has limited application in *in vivo* studies due to the blue emission of TPE. In this regard, a new probe with red-shifted emission was synthesized by conjugating DEVD peptides to an orange emissive tetraphenylethene pyridinium (PyTPE) fluorogen.[21] This probe showed specific light-up responses towards caspase-3 and -7 with 43- and 36-fold fluorescence enhancement, respectively. To test the probe in living animals, **DEVD-PyTPE** was injected subcutaneously into C6 tumor-bearing mice with and without staurosporine (STS, an apoptosis inducer) treatment. Evident fluorescence signals were collected in the STS-treated tumor region with higher brightness than those without STS treatment. The probe was further demonstrated for *ex vivo* assessment of apoptosis induced drug efficacy.

It is known that enzyme–substrate interactions are highly conformation sensitive and reaction kinetics are subject to subtle difference in binding affinities. The effect of isomerization on the probe-enzyme interaction was subsequently studied using dual-functionalized **TPE-2DEVD** probes in *E*- and *Z*-isomers.[22] The synthesized ***E*-TPE-2DEVD** and ***Z*-TPE-2DEVD** probes could be easily separated using HPLC due to a large difference in retention time. It is interesting that both probes showed specific light-up response to caspase-3, but in different manners. The reaction with the

***E*-TPE-2DEVD** probe reached a steady state much more rapidly while ***Z*-TPE-2DEVD** could induce fluorescence light-up ~4 times higher than its *E*-counterpart. Molecular modelling revealed that the ***E*-TPE-2DEVD** probe could yield more favourable binding models with caspase-3, indicating better reactivity for the probe. The higher fluorescence turn-on for ***Z*-TPE-2DEVD** was attributed to the generation of a more hydrophobic product which formed more emissive aggregates in aqueous medium. The ***Z*-TPE-2DEVD** was reckoned to be a more effective probe due to its higher SNR and was successfully applied for apoptosis imaging.

By attaching a target-specific ligand to the above apoptosis probes, they can be transformed into a versatile tool for apoptosis imaging in specific cells, which are useful for disease diagnosis and evaluation of therapeutic effects. Fig. 5 illustrates such an example. As shown in Fig. 5A, TPS is dual-functionalized with a DEVD substrate and cRGD for targeting integrin over-expressed cancer cells.[23] Upon entering specific cells *via* receptor mediated uptake, the probe was cleaved by caspase-3/7 upon apoptosis activation, producing highly emissive products in the aggregated state. Compared to the probe of **DEVD-TPS**, the conjugation of cRGD on the probe further reduced the background signal due to improved water solubility. The effect of targeting and apoptosis imaging was illustrated using both U87-MG and MCF-7 cells. From Fig. 5B and F, the healthy cells appear dark under a confocal microscope after incubation with the probe **DEVD-TPS-cRGD**. Upon pretreatment of the cells with STS, the apoptotic cells were lit up, with a much stronger signal for U87-MG cells (Fig. 5C) than that for MCF-7 cells (Fig. 5G). Both pretreatment of U87-MG cells with caspase inhibitor (Fig. 5D) and blocking of integrin receptors on cell membranes (Fig. 5E) significantly reduced the fluorescent signals in cells. This light-up probe can be further modified with prodrug elements for monitoring therapeutic effects, which will be discussed in the next section.

3.3.4 Image-guided chemotherapy. One of the key challenges in the development of theranostic probes is to effectively deliver the drugs to desired locations with minimum systemic toxicity. Meanwhile, the probe should offer the ability of real-time tracking of drugs and *in situ* monitoring of drug efficacy, which will aid early evaluation of therapeutic effects and reduce the ineffective period of drug acting course.

Liu's group has demonstrated such a theranostic probe with a platinum (Pt)-based prodrug for tracking of drug delivery/release in targeted cells and subsequent imaging of apoptosis induced by drug activation.[24] Cisplatin (cisdichlorodiammine-platinum(II)) is one of the most well-known anti-cancer drugs. It works by crosslinking DNA to ultimately trigger apoptosis. To minimize the side effects caused by this highly toxic drug, its nontoxic form Pt(IV) complexes are usually used as a prodrug which can be reduced to Pt(II) form during activation in cells.[25] As shown in Fig. 6A, the theranostic probe **TPS-DEVD-Pt-cRGD** was synthesized by functionalization of the prodrug containing

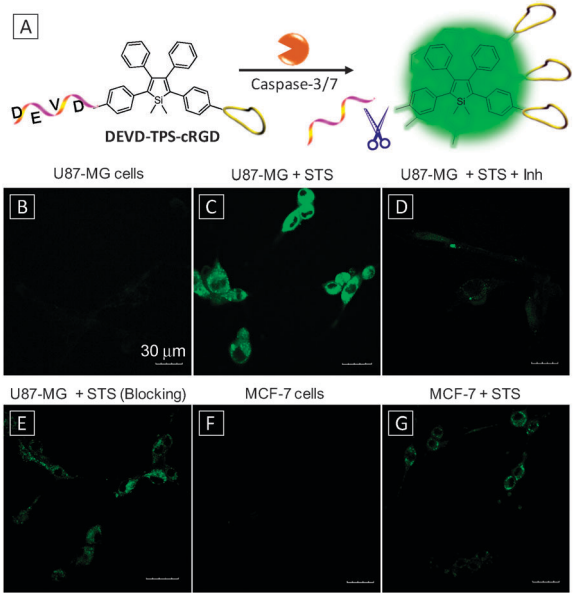

Fig. 5 (A) Schematic illustration of apoptosis imaging in target cells using **DEVD-TPS-cRGD** probe. Confocal fluorescence images of healthy (B) and apoptotic (C) U87-MG cells after incubation with the **DEVD-TPS-cRGD** probe. (D) Apoptotic U87-MG cells pretreated with a caspase-3/7 inhibitor before adding STS. (E) Apoptotic U87-MG cells pretreated with 10 μM cRGD before treatment with **DEVD-TPS-cRGD** and STS. Healthy (F) and apoptotic (G) MCF-7 cells after incubation with the **DEVD-TPS-cRGD** probe. [**DEVD-TPS-cRGD**] = 5 μM, [STS] = 1 μM, [inhibitor, Inh] = 10 μM. Scale bar: 30 μm. Adapted from ref. 23, and reprinted with permission from The Royal Society of Chemistry 2014.

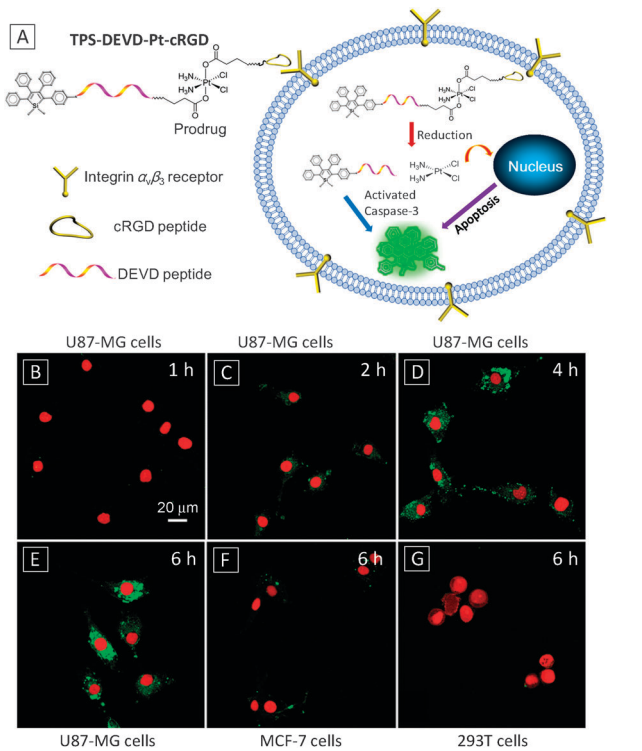

Fig. 6 (A) Schematic illustration of the targeted theranostic Pt(IV) prodrug with an AIE light-up apoptosis sensor for *in situ* early evaluation of its therapeutic effects. (B–E) Real-time confocal fluorescence images of the apoptotic process of U87-MG cells upon treatment with 5 μM **TPS-DEVD-Pt-cRGD** probe. MCF-7 (F) and 293T (G) cells after treatment with 5 μM TPS-DEVD-Pt-cRGD for 6 h. Nuclei were live stained with DRAQ5. Scale bar: 20 μm. Adapted from ref. 24, and reprinted with permission from American Chemical Society 2014.

two NHS groups at its axial positions with an amine-containing apoptosis probe **TPS-DEVD** and a targeting peptide cRGD. Upon selective uptake by integrin overexpressed cells, the probe was reduced by a cell abundant reducing agent such as ascorbic acid to yield separated **TPS-DEVD** and Pt(II) species. The toxic Pt(II) species further induced apoptosis, which was detected by the **TPS-DEVD** probe to yield light-up response. The fluorescence intensity of the probe showed a linear response against caspase-3 concentration, with a detection limit of 1 pM. Fig. 6B–E are confocal images of U87-MG cells upon incubation with **TPS-DEVD-Pt-cRGD** over a period of 6 h, showing progressive light-up of the cells. In contrast, low fluorescence was collected for MCF-7 or 293T cells with a low level of integrin expression even after 6 h. It was found that the viability for U87-MG cells dropped significantly with increasing probe concentration, while little change was observed for the MCF-7 cell. These results indicated that the probe could be selectively uptaken by U87-MG cells and the therapeutic effect of the released drug was successfully visualized by imaging cell apoptosis.

Although the above probe only lights up upon cell apoptosis, which is useful for assessment of the therapeutic effect, it gives no information on the process of drug activation. To capture the dynamic moment of Pt(IV) prodrug activation, a target specific probe was designed with PyTPE conjugated directly with the Pt(IV) prodrug and cRGD (Scheme 5).[26] Five units of Ds were inserted in between Pt(IV) and cRGD to endow the probe with good water-solubility. The probe selectively entered integrin overexpressing cells and was cleaved upon Pt(IV) reduction to yield a highly emissive PyTPE residue. This light-up response with high SNR provides a reliable way for quantitative analysis of the prodrug activation to yield the activated Pt(II) drug. As expected, significantly more cell death was observed in MDA-MB-231 cells than MCF-7 cells due to the much higher level of integrin expression for the former.

Doxorubicin (DOX) is another widely used anticancer drug that works by intercalating DNA. A theranostic probe **cRGD-TPE-Pt-DOX** with both DOX and cisplatin was constructed for dual-drug tracking and monitoring of drug activation in target cells (Scheme 6).[27] As the co-administration of cisplatin and DOX was reported to have synergistic anti-cancer effects, such a probe can further improve drug efficacy with minimum side effects.[28] TPE and DOX constitute a perfect energy transfer pair due to the good spectral overlap between the emission of TPE and absorption of DOX. The probe initially emits red color from DOX as the TPE emission is quenched due to energy transfer. Upon drug activation, free DOX will be released and separated from TPE to recover the blue TPE fluorescence. Incubation of varying concentrations of the probe with reducing agents can be used for quantification of prodrug, with a detection limit of 0.1 μM. Fluorescence imaging results showed that the probe accumulated preferably in MDA-MB-231 cells that overexpress integrin receptors. Initially, only strong red emission was observable in the cytoplasm region and a progressively intensifying blue emission from TPE was observed due to drug activation. As the drug activation process proceeded, the released DOX gradually migrated to cell nuclei, which was clearly visible after 6 h incubation. Indeed, the **cRGD-TPE-Pt-DOX** probe showed higher potency than both cisplatin and DOX when they are used individually.

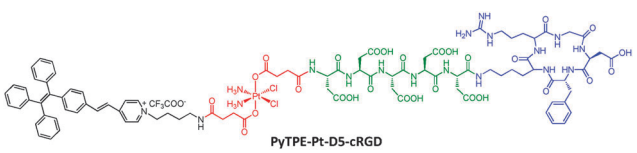

Scheme 5 Chemical structure of the **PyTPE-Pt-D5-cRGD** probe.

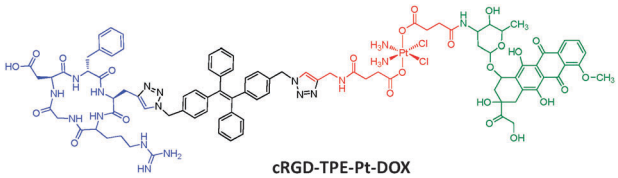

Scheme 6 Chemical structure of the **cRGD-TPE-Pt-DOX** probe.

3.3.5 Image-guided photodynamic therapy. While chemotherapy probes generally rely on a drug moiety to kill cancer cells, the AIEgen itself can be engineered to have therapeutic effects. Photodynamic therapy (PDT) is an emerging therapeutic modality that is useful for non-invasive treatment of malignant tissue/cells.[29] PDT requires a photosensitizer to generate cytotoxic reactive oxygen species (ROS) such as singlet oxygen ($^1O_2$) upon light irradiation. Recently, some AIEgens were found to exhibit photosensitizing characteristics.[30,31] Unlike conventional photosensitizers such as porphyrins, AIEgens do not suffer from decreased photosensitizing efficiency upon aggregation. In one of the studies, a red emissive probe **TPEr-2AP2H** was developed with a photosensitive red TPE derivative and two peptides that could specifically target LAPTM4B protein, a biomarker overexpressed in the majority of tumor cells (Fig. 7A).[31] The introduction of the alkoxyl group and –[PhC=C(CN)$_2$] to TPE red-shifted the emission and the latter group also endowed the probe with photosensitivity for ROS generation. The probe was tested in a number of cancer cell lines (HepG2, HeLa and U2OS) from different origins as well as HEK293 from normal human kidney as a control. The probe was found to localize preferably in cancer cells (Fig. 7B–D) while little signal was observed for control cells (Fig. 7E) due to specific receptor binding by the AP2H peptide of the probe. In addition, the fluorescence of the probe incubated at pH 5.5 was higher than that at pH 7.4, indicating that the probe is useful for sensing a low pH tumor environment. Notably, the PDT efficiency was found to directly correlate with LAPTM4B protein expression levels of modified HEK293 cells, an indication of tumor progression status.

In addition to the PDT probe that can bind surface proteins to generate light-up response, we also proposed a theranostic probe with activatable PDT by intracellular enzyme in target cells.[32] As shown in Scheme 7, the probe consists of a photosensitive TPECM fluorogen with orange emission, which is functionalized with two arms of peptides, comprising a cathepsin B responsive sequence GFLG, a short hydrophilic D_3 sequence for adjusting water solubility and a cRGD ligand for target cell binding. Results showed that the probe could selectively target

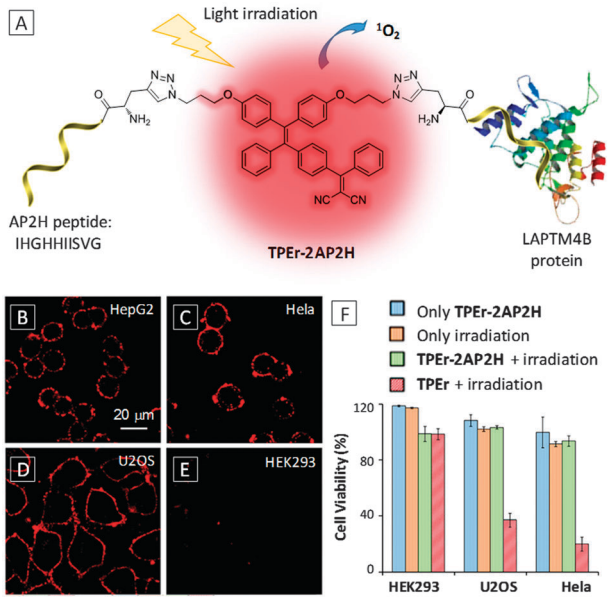

Fig. 7 (A) Schematic illustration of the targeted PDT of the **TPEr-2AP2H** probe. (B–E) Confocal fluorescence images of different cells after incubation with 10 μM **TPEr-2AP2H** in an acidic environment (pH = 5.5). Scale bar: 20 μm. (F) Comparison of cell viability for HEK293, U2OS and HeLa cells under different conditions. [**TPEr-2AP2H**] = [**TPEr**] = 10 μM. Adapted from ref. 31, and reprinted with permission from American Chemical Society 2014.

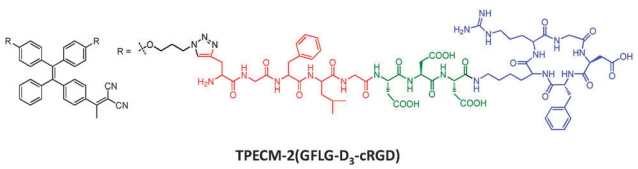

Scheme 7 Chemical structure of the **TPECM-2(GFLG-D_3-cRGD)** probe.

$\alpha_v\beta_3$ integrin overexpressed cancer cells (MDA-MB-231 cells) and localize in cell lysosomes where cathepsin B is enriched. A fluorescence turn-on response was observed in lysosome where the specific cleavage reaction took place between the probe and cathepsin B to yield a highly fluorescent product. The detection limit of cathepsin B was determined to be 0.1 μM in solution. The ROS generation was found to be more effective in the aggregated probe as compared to its molecular dissolved state. The cells with probe enriched lysosomes were then subject to light irradiation and substantial phototoxicity was observed with MDA-MB-231 cells while little was found for control cells. Upon co-staining with a caspase probe (FITC-tagged Annexin V), cell apoptosis was detected only for MDA-MB-231 cells after treatment with the probe and white light irradiation. This probe demonstrates a smart design for targeted and image-guided therapy with concomitant intracellular protein detection ability.

3.4 AIE-small molecule conjugates

3.4.1 Protein sensing. Taking advantage of the specific reaction between enzymes and their small molecule substrates, AIE-small molecule conjugates have been designed to serve as

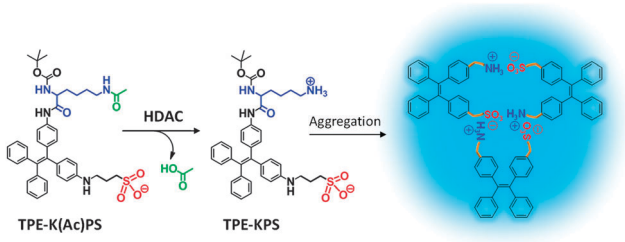

Scheme 8 Chemical structure of the **TPE-K(Ac)PS** probe and the scheme of histone deacetylase detection using the probe.

specific light-up probes for various enzymes based on the cleave-type mechanism. In the following example, a light-up probe for histone deacetylases (HDAC) was constructed by modification of a TPE fluorogen with *N*-α-*t*-butoxycarbonyl-*N*-ε-acetyl-L-lysine (K(Ac)) and propane sulphonic acid (PS) (Scheme 8).[33] The **K(Ac)PS-TPE** probe was almost non-fluorescent due to good water solubility endowed by the anionic sulphonic acid. In the presence of HDAC, the K(Ac)PS group was hydrolysed to primary aliphatic ε-amine (KPS) which was protonated under the reaction conditions. The deacetylation reaction thus yielded a fluorogen product with oppositely charged groups that promoted self-aggregation, which subsequently turned on emission due to AIE activation. The probe was tested with Sirt1, an NAD^+-dependent deacetylase. It was found that significant fluorescence turn-on was observed after the probe was incubated with activated Sirt at 37 °C, while little fluorescence change was detected in the presence of a Sirt inhibitor or at 100 °C, indicating the light-up was due to specific enzymatic reaction between the probe and HDAC.

As compared to charge-induced aggregation illustrated above, a more common strategy relies on generation of hydrophobic products that aggregate in aqueous media. In this regard, AIE probes with phosphate groups were developed for sensing of alkaline phosphatase (ALP).[34,35] Phosphate groups not only served as the substrate of ALP, but also rendered the probe water-soluble and almost non-emissive. Upon incubation with ALP, the phosphate group was cleaved by hydrolysis reaction, yielding a hydrophobic product which emitted strongly in the same media. This light-up response was also used for the study of ALP kinetics to determine kinetic parameters. Based on a similar principle, a TPE probe with two phosphate groups was also designed for the ALP kinetic study as well as ALP quantification in both buffer and serum media.[35] Similarly, a TPE-based probe with four carboxylic ester groups was used for carboxylesterase detection through the formation of supramolecular microfiber aggregates.[36]

A single AIE probe could also be designed to recognize multiple targets *via* different interactions to produce distinct signals. In one example, TPE was functionalized with tetraethylene glycol and phosphate groups.[37] The water-soluble probe not only responded to ALP to generate a hydrophobic product to turn on emission with a greenish color, but also interacted with the positively charged protamine *via* electrostatic interaction to yield micelles with aggregated TPE cores

showing bluish fluorescence. On the other hand, the same type of light-up mechanism can be used for multi-analyte sensing. An AIE probe consisting of a TPE conjugated with four tyrosine units was found to undergo enzyme-catalyzed crosslinking *via* the formation of dityrosine linkages in the presence of horseradish peroxidase (HRP) and hydrogen peroxide (H_2O_2).[38] The enzyme-catalysed coupling led to a significant fluorescence increase and has been exploited for the detection of H_2O_2, an important ROS and biomarker of many different bioprocesses. The assay was further expanded to glucose oxidase catalysed glucose detection and the ELISA kit for antigen detection in the presence of *in situ* generated or added H_2O_2. It is believed that with proper design of conjugated ligands, more versatile probes can be developed for multiplex sensing.

Proteins other than enzymes can generally be detected *via* binding induced aggregation. Scheme 9 illustrates a light-up probe consisting of TPE conjugated with four units of lactosyl groups for detection of cholera toxin (CT), a protein secreted by bacterium *Vibrio cholera*.[39] As CT has five identical B-subunits which can bind lactose, the **TPE-4Lac** probe can interact with CT effectively through multivalent binding, leading to aggregation formation and enhanced emission. Yan and Han also reported sugar-bearing TPE probes for either lectin or glycosidase sensing.[40] Based on the specific binding between mannose and lectin, mannosyl-bearing TPE was used for the detection of lectin Concanavalin A and the study of carbohydrate-protein interaction. In the same work, cellobiosyl-bearing TPE was used as a light-up probe for the study of β-glucosidase hydrolysis using the cleave type mechanism.

3.4.2 Membrane tracking. Membrane is one of the major cell components with a distinctive phospholipid bilayer structure. With proper functionalization, a typical AIEgen can be transformed into a membrane tracker. Zou, Liang and coworkers have synthesized a light-up AIE probe consisting of a TPE conjugated with four arginine units (R_4) and palmitic acid (PA) that can specifically interact with cell membranes (Fig. 8A).[41] The positively charged R_4 served as the targeting ligand for the negatively charged cell membrane while the long alkyl chain in PA was used for membrane insertion, which was conjugated to TPE *via* carboxyl-amine coupling reaction.

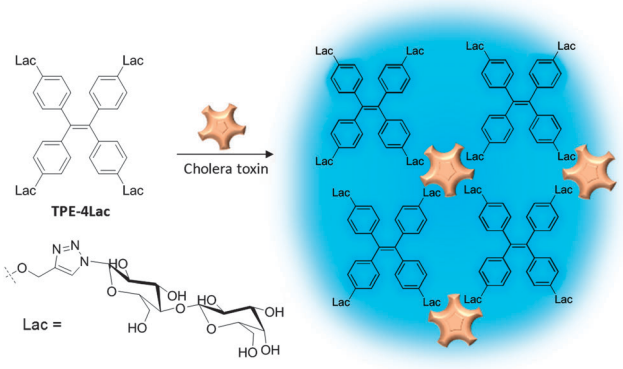

Scheme 9 Chemical structure of the **TPE-4Lac** probe and schematic illustration for cholera toxin detection.

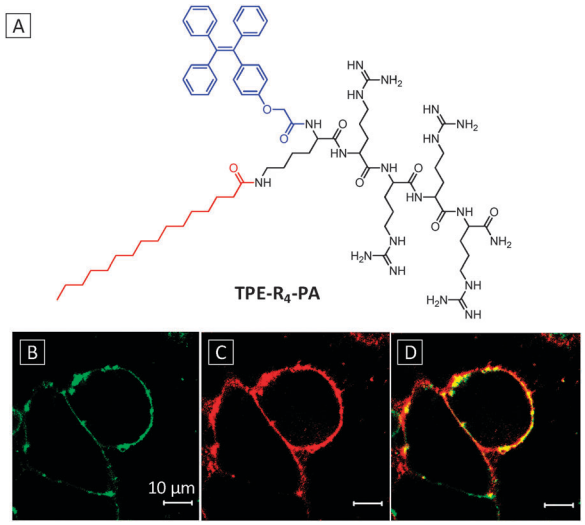

Fig. 8 (A) Chemical structure of **TPE-R_4-PA**. Confocal fluorescence images of live MCF-7 cells stained with 50 μM **TPE-R_4-PA** for 30 min (B) and 10 μM DiI for 10 min (C) at 37 °C. (D) The overlay image of (B) and (C). **TPE-R_4-PA**: λ_{ex} = 405; DiI: λ_{ex} = 543 nm. Scale bar: 10 μm. Adapted from ref. 41, and reprinted with permission from American Chemical Society 2014.

The probe showed enhanced emission at increasing concentration with formation of nanofibers, indicative of self-assembly induced emission. The optimal dosage and incubation time were also investigated for MCF-7 cell membrane tracking. Upon incubating the cells with a 50 μM probe for 30 min, the cell membranes were effectively stained with the **TPE-R_4-PA** probe, which overlaid well with the commercial membrane tracker (1,1′-dioctadecyl-3,3,3′,3′-tetramethylindocarbocyanine perchlorate) (DiI) (Fig. 8B–D). The probe showed much better photostability than DiI, with more than 95% fluorescence intensity retained after 9 min laser excitation. Furthermore, the ability of the probe to be excited by two-photon lasers renders it more attractive for two-photon bioimaging applications.

3.4.3 Mitochondria tracking. Mitochondrion is a vital organelle found in most eukaryotic cells that produces ATP as an energy source for living organisms. In addition to power supply, mitochondrion also plays an important role in cell differentiation, growth, death and signalling. The ability to track mitochondria, especially their real-time morphological and activity changes, is crucial for monitoring biological processes and understanding associated diseases.

As mitochondria have a negative membrane potential, one strategy to target them is to incorporate cationic lipophilic moieties into the probe. Capitalizing on this property, Tang's group has reported an AIE probe for imaging and tracking mitochondria using TPE functionalized with two triphenylphosphonium (TPP), a well-known mitochondria targeting ligand (Fig. 9A).[42] Although carrying positive charges, the probe displayed typical AIE properties. The **TPE-TPP** probe was tested in HeLa cells along with a commercial mitochondria stain MitoTracker Red FM (MT). Confocal images showed that the probe could specially localize in mitochondria with bright blue emission, which

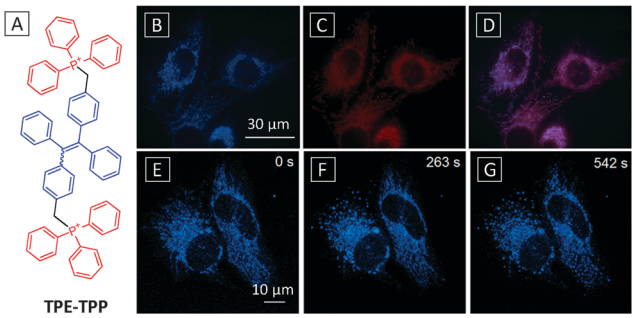

Fig. 9 (A) Chemical structure of the **TPE-TPP** probe. Confocal fluorescence images of HeLa cells stained with 5 μM **TPE-TPP-TPP** for 1 h (B) and MitoTracker Red FM for 15 min (C) and their overlay image (D). Scale bar: 30 μm. (E–G) Time dependent images of CCCP (20 μM) treated live HeLa cells stained with 5 μM **TPE-TPP**. Scale bar: 10 μm. λ_{ex} = 405 nm with filter band pass of 449–520 nm. Adapted from ref. 42, and reprinted with permission from American Chemical Society 2012.

overlapped perfectly with the signal from MT (Fig. 9B–D). As compared to MT, **TPE-TPP** showed much higher resistance to photobleaching. Further studies revealed that **TPE-TPP** showed higher tolerance to membrane potential ($\Delta\psi_m$) reduction than MT with superior sensitivity due to its higher charge density and lipophilicity. Carbonyl cyanide *m*-chlorophenylhydrazone (CCCP) is known to cause dysfunction of ATP synthase and $\Delta\psi_m$ reduction. CCCP pretreated cells incubated with **TPE-TPP** at increasing scanning time are shown in Fig. 9E–G. A clear morphological transformation from reticular to granular is observed for mitochondria, indicating the great potential of the probe for real time mitochondria tracking.

The light-up mechanism for mitochondrial imaging is due to preferential accumulation of the probe in the target organelle. Unlike most light-up probes presented earlier, the **TPE-TPP** mitochondria probe lacks sufficient water solubility and essentially exists as nanoaggregates prior to imaging. Similar examples for mitochondria probes with AIE properties also include a conjugated phosphonium salt synthesized from phosphine-triggered ring-opening of 2,4,5-triphenylpyrylium salt[43] and an orange emissive probe prepared by attachment of a cationic pyridinium unit on a TPE.[44]

Fluorophores with ESIPT characteristics exhibit large Stokes shifts, which are highly desirable for imaging applications. Liu's group demonstrated that by harnessing both AIE and ESIPT properties, a novel mitochondria probe can be constructed for differentiation of brown adipose cells.[45] The probe utilised a salicylaldazine fluorophore with both AIE and ESIPT nature attached with two pyridinium groups for targeting mitochondria (Scheme 10). The probe was almost non-fluorescent in dilute solutions due to free intramolecular rotations. In the aggregated state, the restricted rotation around the N–N bond activated both AIE mechanism and ESIPT, leading to strong emission with a large Stokes shift of 176 nm. The **AIE-Mito** probe was successfully used for staining of mitochondria with good overlap with commercial MT, showing excellent probe retention and very low cytotoxicity. The probe was subsequently used for continuous tracking of mitochondria in differentiating adipose cells over the course of 7 days. Owing to the high SNR and good photostability of the probe, the morphology change of mitochondria from tubular and reticular to punctate was clearly visualized by **AIE-Mito** during the differentiation process.

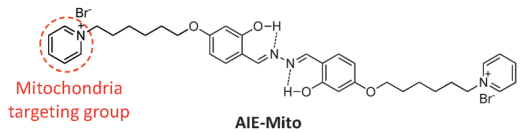

Scheme 10 The chemical structure of mitochondrial tracker **AIE-Mito** with AIE and ESIPT properties.

3.4.4 Lysosome tracking. Lysosome is an enzyme enriched organelle responsible for digesting all kinds of intracellular biomolecules. Tracking of lysosome and esterase activity has great implication in diagnosis of esterase deficient diseases. Based on a similar structure of **AIE-Mito**, a lysosome tracker **AIE-Lyso** with AIE + ESIPT features was constructed by substitution of the hydroxyl group of a salicylaldazine fluorophore with esterase substrates while the end groups were replaced with lysosome targeting morpholine groups (Fig. 10A).[46] The probe was initially non-fluorescent due to blocked hydrogen bonding by acetyl groups and free rotation of N–N which destructed excited-state proton transfer and radiative decay. Upon reaction with esterase, deprotection of the probe led to hydrogen bond formation and activation of ESIPT. This together with the probe accumulation in lysosome activated the AIE mechanism. The probe showed selective light-up

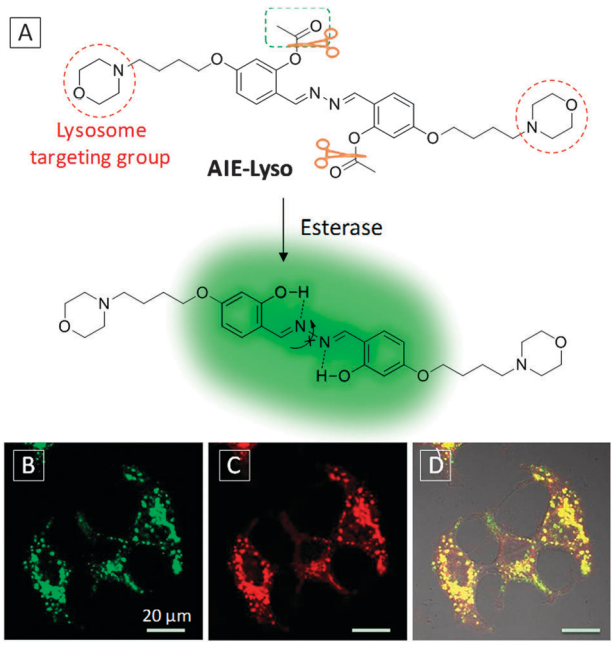

Fig. 10 (A) Chemical structure and reaction scheme of the **AIE-Lyso** probe. Confocal fluorescence images of MCF-7 cells stained with 1.0 mM **AIE-Lyso** (B), or 50 nM LysoTracker Red (C) and their overlay image (D). **AIE-Lyso**: λ_{ex} = 405 nm with filter band pass of 515–560 nm. LysoTracker Red: λ_{ex} = 559 nm with filter band pass of 585–610 nm. Scale bar: 20 μm. Adapted from ref. 46, and reprinted with permission from The Royal Society of Chemistry 2014.

response to esterase in solution, with 70–200 fold higher fluorescence enhancements as compared to other interfering substances, with a detection limit of 2.4×10^{-3} U mL^{-1}. Upon incubation of MCF-7 cells with the **AIE-Lyso** probe, distinct fluorescence signals were observed in lysosome, which overlapped well with the commercial LysoTracker Red signals (Fig. 10B–D). The probe was successfully demonstrated for *in situ* monitoring of esterase activity, showing increased fluorescence intensity over time. The probe was also useful for tracking movements of lysosome in stimulated cells. A similar strategy was applied to design a ratiometric probe using a phosphorylated chalcone derivative with AIE and ESIPT characteristics for ALP sensing and imaging in live cells.[47] As compared to the first two generations, the third generation AIE probes with AIE + ESIPT characteristics have a low background signal despite their limited water solubility, which further reduces the limitation of probe design.

3.4.5 Image-guided therapeutic probes. Typical fluorescence based theranostic probes require labelling of therapeutic agents with fluorescent tags for effective image-guided therapy, which may alter the pharmacokinetics and biodistribution of the drugs. The synthesis of AIEgens with both intrinsic AIE feature and therapeutic function is highly attractive as they do not need additional labelling steps, which can be used to directly visualize the delivery pathway and provide image-guided therapy.

A simple but unique therapeutic probe based on an AIE + ESIPT fluorogen as both imaging reagent and potential chemotherapy drug has recently been reported for image-guided therapy of targeted cancer cells.[48] By replacing the end targeting groups of **AIE-Mito** with TPP (Fig. 11A), the new probe not only accumulated preferably in cancer cell mitochondria, but also exhibited selective cytotoxicity in cancer cells over normal cells. The selectivity was attributed to the more negative membrane potential in cancer cells which tends to attract more positively charged probes. The enriched **AIE-mito-TPP** probe in cancer cell mitochondria formed emissive aggregates due to activation of AIE and ESIPT. In addition, the probe could induce cell stress and mitochondrial dysfunction which subsequently caused cell death to achieve selective killing of cancer cells. Fig. 11B–G show the time-dependent killing of HeLa cells upon incubation with **AIE-mito-TPP** and propidium iodide (PI) dye, a nuclei stain for dead cells. The probe was able to light up mitochondria within 1 h while an increasing amount of PI entered nuclei, indicating progressive cell death. At the 8th h, the overlapped signal between PI and **AIE-mito-TPP** indicated the destruction of nuclei membranes that allowed the probe to enter the nuclei. The probe was found to cause a series of biological changes including decreased mitochondrial membrane potential, elevated intracellular ROS generation, reduced ATP production and inhibited cell growth for HeLa cells.

Liu's group also reported another probe with an AIE + ESIPT feature based on a zinc coordinated salicylaldazine skeleton for apoptosis imaging.[49] **AIE-ZnDPA** was synthesized from the precursor probe **AIE-DPA** and zinc perchlorate hexahydrate (Scheme 11A). **AIE-DPA** and **AIE-ZnDPA** displayed large Stokes shifts of 215 nm and 190 nm, respectively, with no overlap between the absorption and emission spectra. The **AIE-ZnDPA** probe showed weak emission in water and it became highly emissive in water–THF mixtures at THF fractions larger than 80%. Results showed that no staining of **AIE-ZnDPA** was observed for healthy cells while prominent light-up was observed in the membrane region of the cells at early stage apoptosis (Scheme 11B). As early apoptosis is featured by partially exposed phosphatidylserine (PS) on the cell surface, the positively charged probe was able to bind with PS to enhance emission. At the later stage of cell apoptosis whereby

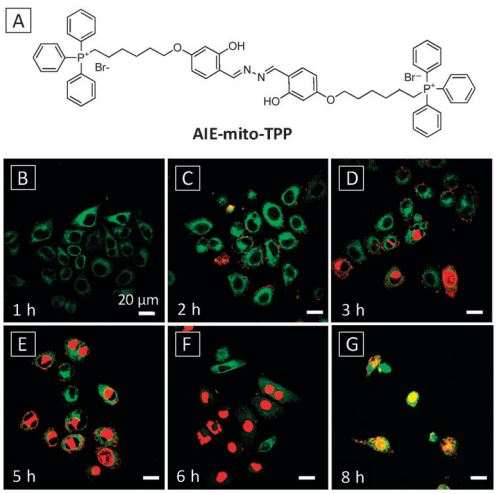

Fig. 11 (A) Chemical structure of **AIE-mito-TPP**. (B–G) Confocal fluorescence images of the staining process of HeLa cells with 2 μM **AIE-mito-TPP** at different incubation time. Nuclei were stained with PI. **AIE-mito-TPP**: λ_{ex} = 405 nm with filter band pass of 510–560 nm. PI: λ_{ex} = 543 nm with filter band pass of 575–625 nm. Scale bar: 20 μm. Adapted from ref. 48, and reprinted with permission from Wiley-VCH 2014.

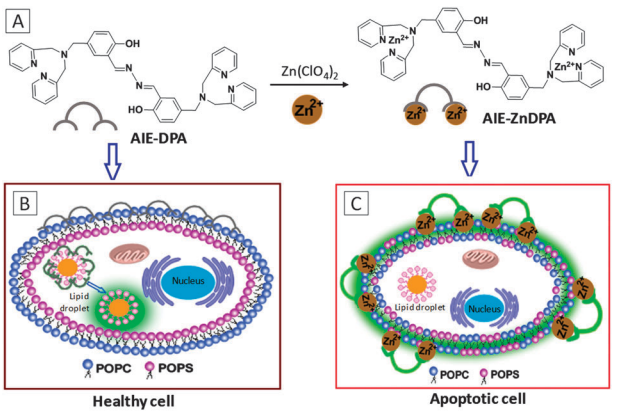

Scheme 11 (A) Reaction scheme of Zn^{2+} chelation of **AIE-DPA** to form the complex of **AIE-ZnDPA**. Schematic illustration of lipid droplet staining in healthy cell using the **AIE-DPA** probe (B) and membrane staining in apoptotic cells using the **AIE-ZnDPA** probe (C). POPC: 1-palmitoyl-2-oleoyl-*sn*-*glycero*-3-phosphocholine (zwitterionic); POPS: 1-palmitoyl-2-oleoyl-*sn*-*glycero*-3-phosphoserine (anionic). POPC and POPS are two major components of cell membrane lipids. Adapted from ref. 49, and reprinted with permission from The Royal Society of Chemistry 2014.

the membrane integrity is completely compromised, the probe was found to light up nuclei specifically. In contrast, **AIE-DPA** was able to stain both live and apoptotic HeLa cells and specifically light up lipid droplets (Scheme 11C). The simple manipulation of the metal ion presence on the probe was able to alter the probe function for different applications.

The same **AIE-ZnDPA** probe also shows the photosensitization effect, which was subsequently applied for selective fluorescence imaging and killing of both Gram-positive and Gram-negative bacteria over mammalian cells.[50] Upon co-incubation of bacteria (Gram-positive *B. Subtilis* or Gram-negative *E. coli*) and mammalian cells (Jurkat T or K562 cells) with the probe, only bacteria were stained by **AIE-ZnDPA**, signalling the activation of AIE and ESPIT mechanisms. The selective staining of bacteria was attributed to the electrostatic interaction between the positively charged probe and the bacteria membrane which has a more negative potential as compared to mammalian cells. The probe was found to kill Gram-positive bacteria even in dark due to depolarization of bacteria membranes. For Gram-negative bacteria, white light irradiation was required to generate ROS for selective photodynamic killing. In both cases, the cells co-incubated showed a little change of viability.

4. Conclusion and outlook

AIEgens are an emerging class of fluorogenic molecules with unique photophysical properties whose biotech applications are attracting increasing attention. In this review, we have presented general strategies for design and synthesis of AIEgen based light-up bioprobes and discussed typical examples of various AIEgen conjugates for biosensing, imaging and image-guided therapy. Through ingenious design of probe structure, light-up response is achieved for sensing a wide variety of bioanalytes including nucleic acids, proteins and small molecules with high SNR. The distinctive near-zero background and highly emissive aggregates of the probes make them possible to realize wash-free sensing and continuous imaging or monitoring of biological processes with good sensitivity and reliability. The design of AIE bioprobes is evolving constantly to adapt to changing analytes and the need for multifunctionality. In the first generation, AIEgens are limited to conjugation with highly hydrophilic recognition elements to achieve a low background. The introduction of a hydrophilic linker to the probe enables hydrophobic recognition elements to be conjugated. These two generations, however, still pose limitations to probe solubility while the adoption of the cooperative ESIPT mechanism provides an effective remedy to further expand the probe design. Additional incorporation of drugs and stimuli responsive elements enables image-guided smart drug delivery and release in targeted cells. The use of AIEgens with intrinsic therapeutic effects can further improve their therapeutic function with minimum modifications and systemic toxicity.

Two aspects are deemed essential for formulating advanced AIE light-up probes. The examples covered in this review mainly used blue and green emissive TPE or TPS fluorogens, which have limited application in *in vivo* studies that require deep penetration and low autofluorescence. One option is to develop AIEgens with multiphoton absorption. The alternative choice is to design red or FR/NIR emissive AIEgens with desirable functionalities, which can greatly widen the scope of their *in vivo* applications. The discovery of AIEgens with high chemotherapeutic or PDT efficiency will drive the development of advanced theranostic platforms with extremely simple design. On the other hand, the conjugation of AIEgens with a more specific and wider range of targeting ligands will yield more selective probes that can potentially target a broader spectrum of biomolecules, cells or organelles in the biosystem. It is also important to note that AIEgens can be assembled into emissive nanoparticles for applications in vascular imaging, cell tracing and molecular probing. The further development of AIEgens with stimuli-responsiveness (*e.g.* photo-, thermo-, vapo-, piezo- and chronochromisms) will find new applications as advanced function indicators, sensors and active materials in optoelectronic devices. On the basis of the current work, we hope to trigger more interest and ideas from researchers and to further promote AIEgens to various biomedical and energy applications.

Acknowledgements

We thank the Ministry of Defence (R279-000-340-232), SMART (R279-000-378-592), the National University of Singapore (R279-000-415-112), Singapore NRF Investigatorship and the A-Star Joint Council Office (IMRE/14-8P1110), the Research Grants Council of Hong Kong (HKUST2/CRF/10), the Ministry of Science and Technology of China (973 program 2013CB834701) and Guangdong Innovative Research Team Program (201101C0105067115) for financial support.

Notes and references

1 X. Li, X. Gao, W. Shi and H. Ma, *Chem. Rev.*, 2013, **114**, 590–659.
2 E. Lacivita, M. Leopoldo, F. Berardi, N. A. Colabufo and R. Perrone, *Curr. Med. Chem.*, 2012, **19**, 4731–4741.
3 J. Guo, J. Ju and N. Turro, *Anal. Bioanal. Chem.*, 2012, **402**, 3115–3125.
4 M. Wang, G. Zhang, D. Zhang, D. Zhu and B. Z. Tang, *J. Mater. Chem.*, 2010, **20**, 1858–1867.
5 D. Ding, K. Li, B. Liu and B. Z. Tang, *Acc. Chem. Res.*, 2013, **46**, 2441–2453.
6 J. Luo, Z. Xie, J. W. Y. Lam, L. Cheng, H. Chen, C. Qiu, H. S. Kwok, X. Zhan, Y. Liu, D. Zhu and B. Z. Tang, *Chem. Commun.*, 2001, 1740–1741.
7 Y. Hong, J. W. Y. Lam and B. Z. Tang, *Chem. Soc. Rev.*, 2011, **40**, 5361–5388.
8 Z. Y. Yang, Z. G. Chi, T. Yu, X. Q. Zhang, M. N. Chen, B. J. Xu, S. W. Liu, Y. Zhang and J. R. Xu, *J. Mater. Chem.*, 2009, **19**, 5541–5546.
9 G. T. Hermanson, *Bioconjugate Techniques*, Academic Press, Rockford, Illinois, USA, 2008.

10 J. E. Kwon and S. Y. Park, *Adv. Mater.*, 2011, **23**, 3615–3642.
11 Y. Li, Y. Wu, J. Chang, M. Chen, R. Liu and F. Li, *Chem. Commun.*, 2013, **49**, 11335–11337.
12 H. Wang, J. Liu, A. Han, N. Xiao, Z. Xue, G. Wang, J. Long, D. Kong, B. Liu, Z. Yang and D. Ding, *ACS Nano*, 2014, **8**, 1475–1484.
13 S. Li, S. M. Langenegger and R. Haner, *Chem. Commun.*, 2013, **49**, 5835–5837.
14 Y. Li, R. T. K. Kwok, B. Z. Tang and B. Liu, *RSC Adv.*, 2013, **3**, 10135–10138.
15 X. Lou, C. W. T. Leung, C. Dong, Y. Hong, S. Chen, E. Zhao, J. W. Y. Lam and B. Z. Tang, *RSC Adv.*, 2014, **4**, 33307–33311.
16 H. Shi, J. Liu, J. Geng, B. Z. Tang and B. Liu, *J. Am. Chem. Soc.*, 2012, **134**, 9569–9572.
17 Y. Huang, F. Hu, R. Zhao, G. Zhang, H. Yang and D. Zhang, *Chem. – Eur. J.*, 2014, **20**, 158–164.
18 R. Zhang, Y. Yuan, J. Liang, R. T. K. Kwok, Q. Zhu, G. Feng, J. Geng, B. Z. Tang and B. Liu, *ACS Appl. Mater. Interfaces*, 2014, **6**, 14302–14310.
19 Y. Yuan, R. T. K. Kwok, G. Feng, J. Liang, J. Geng, B. Z. Tang and B. Liu, *Chem. Commun.*, 2014, **50**, 295–297.
20 H. Shi, R. T. K. Kwok, J. Liu, B. Xing, B. Z. Tang and B. Liu, *J. Am. Chem. Soc.*, 2012, **134**, 17972–17981.
21 H. Shi, N. Zhao, D. Ding, J. Liang, B. Z. Tang and B. Liu, *Org. Biomol. Chem.*, 2013, **11**, 7289–7296.
22 J. Liang, H. Shi, R. T. K. Kwok, M. Gao, Y. Yuan, W. Zhang, B. Z. Tang and B. Liu, *J. Mater. Chem. B*, 2014, **2**, 4363–4370.
23 D. Ding, J. Liang, H. Shi, R. T. K. Kwok, M. Gao, G. Feng, Y. Yuan, B. Z. Tang and B. Liu, *J. Mater. Chem. B*, 2014, **2**, 231–238.
24 Y. Yuan, R. T. K. Kwok, B. Z. Tang and B. Liu, *J. Am. Chem. Soc.*, 2014, **136**, 2546–2554.
25 X. Wang and Z. Guo, *Chem. Soc. Rev.*, 2013, **42**, 202–224.
26 Y. Yuan, Y. Chen, B. Z. Tang and B. Liu, *Chem. Commun.*, 2014, **50**, 3868–3870.
27 Y. Yuan, R. T. K. Kwok, R. Zhang, B. Z. Tang and B. Liu, *Chem. Commun.*, 2014, **50**, 11465–11468.
28 J. T. Thigpen, M. F. Brady, H. D. Homesley, J. Malfetano, B. DuBeshter, R. A. Burger and S. Liao, *J. Clin. Oncol.*, 2004, **22**, 3902–3908.
29 A. Yuan, J. Wu, X. Tang, L. Zhao, F. Xu and Y. Hu, *J. Pharm. Sci.*, 2013, **102**, 6–28.
30 Y. Yuan, G. Feng, W. Qin, B. Z. Tang and B. Liu, *Chem. Commun.*, 2014, **50**, 8757–8760.
31 F. Hu, Y. Huang, G. Zhang, R. Zhao, H. Yang and D. Zhang, *Anal. Chem.*, 2014, **86**, 7987–7995.
32 Y. Yuan, C.-J. Zhang, M. Gao, R. Zhang, B. Z. Tang and B. Liu, *Angew. Chem., Int. Ed.*, 2015, **54**, 1780–1786.
33 K. Dhara, Y. Hori, R. Baba and K. Kikuchi, *Chem. Commun.*, 2012, **48**, 11534–11536.
34 X. Gu, G. Zhang, Z. Wang, W. Liu, L. Xiao and D. Zhang, *Analyst*, 2013, **138**, 2427–2431.
35 J. Liang, R. T. K. Kwok, H. Shi, B. Z. Tang and B. Liu, *ACS Appl. Mater. Interfaces*, 2013, **5**, 8784–8789.
36 X. Wang, H. Liu, J. Li, K. Ding, Z. Lv, Y. Yang, H. Chen and X. Li, *Chem. – Asian J.*, 2014, **9**, 784–789.
37 Z. Song, Y. Hong, R. T. K. Kwok, J. W. Y. Lam, B. Liu and B. Z. Tang, *J. Mater. Chem. B*, 2014, **2**, 1717–1723.
38 X. Wang, J. Hu, G. Zhang and S. Liu, *J. Am. Chem. Soc.*, 2014, **136**, 9890–9893.
39 X.-M. Hu, Q. Chen, J.-X. Wang, Q.-Y. Cheng, C.-G. Yan, J. Cao, Y.-J. He and B.-H. Han, *Chem. – Asian J.*, 2011, **6**, 2376–2381.
40 J.-X. Wang, Q. Chen, N. Bian, F. Yang, J. Sun, A.-D. Qi, C.-G. Yan and B.-H. Han, *Org. Biomol. Chem.*, 2011, **9**, 2219–2226.
41 C. Zhang, S. Jin, K. Yang, X. Xue, Z. Li, Y. Jiang, W.-Q. Chen, L. Dai, G. Zou and X.-J. Liang, *ACS Appl. Mater. Interfaces*, 2014, **6**, 8971–8975.
42 C. W. T. Leung, Y. Hong, S. Chen, E. Zhao, J. W. Y. Lam and B. Z. Tang, *J. Am. Chem. Soc.*, 2012, **135**, 62–65.
43 W. Chen, D. Zhang, W. Gong, Y. Lin and G. Ning, *Spectrochim. Acta, Part A*, 2013, **110**, 471–473.
44 N. Zhao, M. Li, Y. Yan, J. W. Y. Lam, Y. L. Zhang, Y. S. Zhao, K. S. Wong and B. Z. Tang, *J. Mater. Chem. C*, 2013, **1**, 4640–4646.
45 M. Gao, C. K. Sim, C. W. T. Leung, Q. Hu, G. Feng, F. Xu, B. Z. Tang and B. Liu, *Chem. Commun.*, 2014, **50**, 8312–8315.
46 M. Gao, Q. Hu, G. Feng, B. Z. Tang and B. Liu, *J. Mater. Chem. B*, 2014, **2**, 3438–3442.
47 Z. Song, R. T. K. Kwok, E. Zhao, Z. He, Y. Hong, J. W. Y. Lam, B. Liu and B. Z. Tang, *ACS Appl. Mater. Interfaces*, 2014, **6**, 17245–17254.
48 Q. Hu, M. Gao, G. Feng and B. Liu, *Angew. Chem., Int. Ed.*, 2014, **53**, 14225–14229.
49 Q. Hu, M. Gao, G. Feng and B. Liu, *ACS Appl. Mater. Interfaces*, 2014, DOI: 10.1021/am508838z.
50 M. Gao, Q. Hu, N. Tomczak, R. Liu, G. Feng, B. Xing, B. Z. Tang and B. Liu, *Adv. Healthcare Mater.*, 2014, DOI: 10.1002/adhm.201400654.